Research Square

Preprints are preliminary reports that have not undergone peer review.
They should not be considered conclusive, used to inform clinical practice,
or referenced by the media as validated information.

Time course of Fto mRNA and FTO protein abundance in mouse inner medullary collecting duct cells exposed to hypertonicity

Xiaoyun Liao[1]

448271699@qq.com

Jinan University

Cuijuan Luo[1]

Jinan University

Pei Long[1]

Jinan University

Short Report

Keywords: Kidney Medulla, Collecting Kidney Tubules, Osmotic Pressure, HSP70 Heat-Shock Proteins, RNA Demethylases, Gene Expression Regulation

Posted Date: November 25th, 2026

DOI: https://doi.org/10.21203/rs.3.rs-11800351/v1

License: This work is licensed under a Creative Commons Attribution 4.0 International License.
Read Full License

Additional Declarations: No competing interests reported.

Abstract

Objective: To characterize the time courses of *Fto* mRNA and FTO protein abundance in mouse inner medullary collecting duct cells exposed to hypertonic medium (550 mOsm/kg H_2O) and to examine their relationship with heat shock protein 70 (HSP70) abundance.
Results: Across three independent biological replicates, *Fto* mRNA abundance declined at intermediate time points and partially recovered by 10 h. Mean FTO protein abundance showed a modest upward trend, and HSP70 abundance showed a larger increase at later time points. Under isotonic conditions, HSP70 overexpression and knockdown were accompanied by higher and lower mean FTO abundance, respectively. FTO overexpression was accompanied by a modest increase in mean HSP70 abundance, and FTO knockdown by a decrease. During hypertonic exposure, FTO abundance did not consistently increase with HSP70 overexpression. The time courses showed distinct patterns for *Fto* mRNA and FTO protein. Whether FTO and HSP70 directly regulate each other or contribute to cytoprotection remains to be determined.

Introduction

Renal medullary cells adapt to changing extracellular tonicity through transcriptional and post-transcriptional responses. NFAT5 regulates osmotic adaptation [1], with recent studies defining nuclear trafficking, ionic-strength sensing and renal transcriptional programs [2–4]. HSP70 is induced through TonEBP/NFAT5 [5]. Our previous work identified tonicity-responsive miR-23a-5p targeting HSPA1B in renal cells [6].

FTO demethylates RNA N6-methyladenosine (m6A) [7]. Heat-stress studies connect RNA methylation with selective Hsp70 translation [8, 9], while arsenite experiments link m6A-dependent interactions to stress-granule stability [10]. Whether related expression responses occur during hypertonicity remains incompletely characterized. We examined Fto transcript and FTO/HSP70 protein time courses in mIMCD3 cells, reciprocal expression changes following protein perturbation, and HSP70 perturbation during hypertonic exposure.

Main text

Materials and methods: Cell culture and exposure

mIMCD3 cells (ATCC CRL-2123; Manassas, VA, USA) were cultured in DMEM (11965-092) with 10% fetal bovine serum (10099-141; Gibco, Thermo Fisher Scientific, Grand Island, NY, USA), 100 U/mL penicillin and 100 µg/mL streptomycin at 37°C and 5% CO2. Cells were used within 15 passages; quarterly PCR-based mycoplasma tests were negative. Medium osmolality was increased from 300 to 550 mOsm/kg H2O using sterile 5 mol/L NaCl and verified with an Osmomat 030 osmometer (Gonotec, Berlin, Germany).

Untransfected cells were sampled at 0, 0.5, 1, 2, 4, 6, 8 and 10 h. HSP70 perturbation time courses comprised 0, 2 and 6 h, starting 48 h after transfection. Only pretreatment 0 h controls were available; time-matched isotonic controls were absent. Separate isotonic perturbation experiments were harvested 48 h after transfection.

Cultures were maintained using a Thermo 371 incubator and Thermo 1384 safety cabinet (Thermo Fisher Scientific, Waltham, MA, USA). Morphology was monitored with a ZEISS AXIO Vert Z1 microscope (Carl Zeiss, Oberkochen, Germany). Osmolality was verified immediately after preparation of each medium batch. Exposure timing began when isotonic medium was replaced by hypertonic medium; the 0 h samples were collected before replacement.

Quantitative PCR

RNA was isolated using RNAiso Plus (D9108A; TaKaRa, Dalian, China), treated with DNase I and assessed with a NanoDrop 2000 (Thermo Fisher Scientific, Waltham, MA, USA). RNA (100–500 ng) was reverse-transcribed using M-MLV (D2639A; TaKaRa), random hexamers and oligo(dT), in 10 µL at 37°C for 15 min, 42°C for 60 min and 75°C for 10 min.

PCR used GoTaq Hot Start Polymerase (Promega, Madison, WI, USA), SYBR Green I (Thermo Fisher Scientific) and an ABI StepOnePlus (Applied Biosystems, Foster City, CA, USA). Reactions (20 µL) underwent 95°C for 180 s, then 40 cycles of 95°C for 10 s and 60°C for 30 s, followed by melting-curve analysis. Fto primers were 5'-GAAGCTAAGAAACTGAGGCT-3' and 5'-TTCAGCTGCCACTGCTGATAG-3'; Rpl14 primers were 5'-GGCTTTAGTGGATGGACCCT-3' and 5'-ATTGATATCCGCCTTCTCCC-3' (Guangzhou Aiji Biotechnology, Guangzhou, China). Relative expression was calculated as 2^(−ΔΔCt), with ΔCt = Ct(Fto) − Ct(Rpl14) and ΔΔCt = ΔCt(sample) − ΔCt(0 h) [11]. Each biological experiment used its corresponding 0 h sample on the same plate. Technical wells were summarized within samples.

Plasmid transfection

The OmicsLink shRNA constructs (GeneCopoeia) used the psi-LVRH1GP backbone. The shRNA-FTO construct (MSH030680-LVRH1GP-a, clone OS611560) targeted mouse Fto (NM_011936.2, 5'-GGTTTCAAGGCAATCGATACA-3'). The shRNA-HSP70 construct (MSH029409-LVRH1GP-a, clone OS608034) targeted mouse Hspa1b (NM_010478.2, 5'-CCGATTACTGTCAAGGTTATT-3'). The non-targeting control was CSHCTR001-LVRH1GP (clone OSNEG20, 5'-GCTTCGCGCCGTAGTCTTA-3').

LV125-FTO and LV125-HSP70 plasmids were compared with matched LV125-Control; shRNA-FTO and shRNA-HSP70 were compared with a non-targeting shRNA control (shRNA-Control). The FTO overexpression construct encoded mouse Fto (GeneCopoeia, catalog no. EX-Mm21381-Lv125, RefSeq NM_011936). The matched overexpression control expressed EGFP (GeneCopoeia, catalog no. EX-EGFP-Lv125). The HSP70 overexpression construct (LV125-HSP70) encoded mouse Hspa1b (GeneCopoeia, catalog no. EX-Mm30347-Lv125, RefSeq NM_010478). Mouse coding-sequence constructs were

introduced by transient plasmid transfection, without viral packaging or transduction. Immunoblot results are reported as HSP70 because the assay did not distinguish individual HSP70 isoforms.

Cells at 70–80% confluence received DNA and PEI (Geneup, China) at a 1:3 mass ratio. Six-well cultures received 2 μg DNA for RNA collection and twelve-well cultures 1 μg for protein collection (plates: Corning, Corning, NY, USA). Complexes formed for 10–15 min; medium was replaced after 6 h. Candidate shRNAs were screened before selection. Treatment and matched control cultures were processed in parallel within each biological experiment.

Immunoblotting and normalization

Cells were lysed in RIPA buffer with protease inhibitors (Roche, Mannheim, Germany) on ice for 30 min and centrifuged at 12,000 × g for 5 min at 4°C. Protein concentrations were measured by Pierce BCA assay (Thermo Fisher Scientific). Proteins (20 μg/lane) underwent SDS-PAGE (Bio-Rad, Hercules, CA, USA) and PVDF transfer. After blocking in 5% milk/TBST for 1 h, membranes were incubated overnight at 4°C with FTO (Abcam, Cambridge, UK; ab92821; 1:1,000), HSP70 (Cell Signaling Technology, Danvers, MA, USA; 4872; 1:1,000) or β-actin (Sigma-Aldrich, St. Louis, MO, USA; A5441; 1:10,000) antibodies. HRP-conjugated secondary antibodies (Cell Signaling Technology; 7074/7076; 1:5,000) were applied for 1 h. Pierce ECL (32209; Thermo Fisher Scientific) signals were captured with a Tanon-5200 (Tanon, Shanghai, China).

ImageJ v1.53 (NIH, Bethesda, MD, USA) quantified integrated densities after subtraction of mean adjacent background intensity multiplied by band area. Only nonsaturated exposures were quantified. Each target signal was divided by its matched β-actin signal. Untransfected time courses were calibrated to 0 h; isotonic perturbation experiments to their matched vector or shRNA controls. For biological replicates 2 and 3 in Fig. 3C and D, the same sample lysates were run on a separate gel and transferred to a new membrane for β-actin detection. FTO and HSP70 band intensities were normalized to the β-actin signal matched by sample identity from these later blots (Additional file 1).

For hypertonic perturbation experiments, both LV-Control and LV-HSP70 groups were calibrated to the LV-Control 0 h value for the same target protein within the corresponding experiment. Both sh-Control and sh-HSP70 groups were similarly calibrated to sh-Control 0 h. Thus, relative abundance = (target/β-actin)sample ÷ (target/β-actin)matched control at 0 h. Intervention-group 0 h values were not fixed at 1. FTO and HSP70 were calibrated separately; their numerical fold changes do not compare absolute abundance between proteins.

Band and background regions had identical dimensions within each image. Lanes from a given image were acquired under identical exposure settings, and uncropped exposures and loading records were retained. Common calibration was applied separately to each biological experiment before summary statistics were calculated. The reference for a 2 or 6 h intervention sample remained control 0 h, rather

than control at the same time point. Consequently, a plotted value combines the baseline difference and subsequent temporal change; it is not itself a time-specific intervention-to-control ratio.

Data analysis

Three independent culture, treatment and harvest experiments were performed (n = 3). GraphPad Prism 9.0 (GraphPad Software, San Diego, CA, USA) was used for plotting means ± SEM. Each point represents one biological experiment. Analyses were descriptive; no inferential tests were performed. Control values fixed at 1 reflect calibration, not absent biological variability. Common-control calibration preserves relative baseline differences between intervention and control groups within each experiment.

Results

Transcript and protein time courses

Fto mRNA showed an intermediate decline with partial recovery at 10 h (Fig. 1A). Early measurements were more dispersed; means at 2–8 h remained below baseline. Protein quantification indicated a modest upward FTO trend and a larger late HSP70 increase (Fig. 1B,C), differing descriptively from the transcript profile. HSP70 measurements were newly performed for this study; induction was consistent with our previous report [6].

At 10 h, mean Fto transcript abundance remained below the pretreatment reference despite its recovery from the intermediate-time values. The larger HSP70 fold response provides a stress-response comparator, but the separate normalization of each protein prevents inference that HSP70 molecules were more abundant than FTO molecules. No claim of statistical significance is made for these temporal differences.

Reciprocal perturbation under isotonic conditions

HSP70 overexpression was accompanied by higher mean FTO abundance (Fig. 2A,C), whereas HSP70 knockdown was accompanied by lower mean FTO abundance (Fig. 2B,D). FTO overexpression was associated with a smaller increase in mean HSP70 abundance (Fig. 2E,G), and FTO knockdown with lower HSP70 abundance (Fig. 2F,H). These associated changes suggest an expression relationship without establishing direct regulation.

HSP70 perturbation during hypertonic exposure

With calibration to matched control 0 h, HSP70 abundance was already higher in the overexpression group before hypertonic exposure (Fig. 3A,C). HSP70 increased at later times, with substantial variability at 6 h. FTO did not show a consistent enhancement in the HSP70-overexpression background across the sampled times.

In the knockdown series, HSP70 remained lower in the sh-HSP70 group than in its matched control, while FTO showed different temporal profiles and appreciable dispersion at 6 h (Fig. 3B,D). Common-control calibration permits descriptive comparison of relative abundance, including baseline differences. However, these observations do not establish that HSP70 promotes FTO accumulation during hypertonic exposure.

Discussion

The principal observations were an intermediate decline in Fto mRNA, a different aggregate FTO protein profile and associated expression changes after reciprocal perturbation under isotonic conditions. The hypertonic intervention series did not show a consistent enhancement of FTO with HSP70 overexpression. These results frame an exploratory expression study rather than a demonstrated regulatory pathway.

Transcript–protein discordance can reflect temporal delays, translation or turnover. Integrated measurements illustrate their distinct contributions [12]. Hypoxia experiments also show stress-dependent FTO localization and degradation [13], but these mechanisms cannot be assigned to the present hypertonic model. Lower transcript abundance alongside higher protein quantification does not itself establish enhanced translation or stabilization.

HSP70 induction is consistent with osmotic adaptation [5]; the rate of osmotic elevation also influences this response [14]. Shared responses to hypertonicity nevertheless do not establish a regulatory relationship. Reciprocal perturbation provides additional evidence of associated expression changes, but off-target effects or altered cellular state remain possible. Independent targeting sequences and rescue experiments would strengthen specificity.

The isotonic intervention experiments and hypertonic time courses address different questions. Associated protein changes after 48 h of transfection under isotonic conditions cannot automatically be extrapolated to cells subsequently exposed to 550 mOsm/kg H2O. Changes in baseline expression may also influence the apparent fold response. This context dependence motivates reporting the two experimental settings separately, without combining them into a single directional mechanism.

Common-control 0 h normalization retains baseline differences. Accordingly, higher HSP70 in the overexpression group at 0 h reflects a difference preceding exposure, rather than an additional hypertonic response. Baseline abundance, changes over time and intervention-dependent responses are distinct comparisons. An intervention-by-time analysis preserving biological batch structure would be required to test response modification; even a significant interaction would not establish direct regulation. The present descriptive analysis cannot establish either an effect or equivalence between groups.

Heat-stress findings connecting FTO-related RNA methylation and Hsp70 translation provide mechanistic context [8, 9]. FTO substrate use depends on RNA context and localization, including

internal m6A and cap-adjacent m6Am [15–17]. Recent work further defines cap recognition [18], while nitric oxide can inhibit catalytic activity [19]. Protein abundance therefore cannot substitute for enzymatic activity. Methylation, physical interaction, translation rates and turnover were not measured here.

Limitations

These findings describe the first 10 h after a single NaCl challenge in mIMCD3 cells. Comparison with the pretreatment baseline leaves the contributions of elapsed culture time and medium exchange unresolved. The magnitude of the Fto transcript change also depends on assumptions about amplification efficiency and Rpl14 stability [20]. With three independent experiments, the size of the modest FTO protein change remains uncertain. Separate β-actin blots for two replicates in the hypertonic perturbation series may introduce additional gel-to-gel and transfer variability.

The reciprocal expression changes under isotonic conditions raise the possibility that FTO and HSP70 respond to a shared change in cell state. During hypertonic exposure, HSP70 overexpression produced no consistent increase in FTO across the sampled times. Together, these observations leave open whether either protein directly regulates the other. Protein abundance alone also leaves FTO catalytic activity and the consequences for cell survival unresolved. The findings therefore apply to acute expression responses in this cell line. Their relevance to sustained osmotic adaptation in the intact renal medulla remains to be established.

List of abbreviations

BCA, bicinchoninic acid; Ct, threshold cycle; DMEM, Dulbecco’s modified Eagle medium; FTO, fat mass and obesity-associated protein; HSP70, heat shock protein 70; m6A, N6-methyladenosine; m6Am, N6,2'-O-dimethyladenosine; mIMCD3, mouse inner medullary collecting duct 3; NFAT5, nuclear factor of activated T cells 5; PEI, polyethylenimine; PVDF, polyvinylidene difluoride; RIPA, radioimmunoprecipitation assay; SEM, standard error of the mean; shRNA, short hairpin RNA; TBST, Tris-buffered saline with Tween 20; TonEBP, tonicity-responsive enhancer-binding protein.

Declarations

Ethics approval and consent to participate

This study used only the commercially available mIMCD3 cell line and did not involve human participants, human tissues or experimental animals; ethics committee approval was therefore not required.

Consent for publication

Not applicable.

Competing interests

The authors declare no competing interests.

Supplementary information

Additional file 1 (PDF). Uncropped immunoblots for Figs. 1B, 2A, 2B, 2E, 2F, 3A and 3B. The file includes all three biological replicates and the separate β-actin blots used to normalize replicates 2 and 3 in Fig. 3C and D.

Funding

This work was supported by the Medical Joint Fund of Jinan University (Grant No. YXZY2024006); the Medical Science and Technology Research Fund of Guangdong Province (Grant Nos. A2024684, B2026332, B2026596); and the Science and Technology Project of Heyuan (Social Development Science and Technology Program, Project No. 2022042).

Author Contribution

Xiaoyun Liao: Conceptualization, Investigation, Resources, Data curation, Writing – original draft, Writing – review and editing, Visualization, Funding acquisition. Cuijuan Luo: Resources, Data curation, Writing – review and editing, Funding acquisition. Pei Long: Resources, Writing – review and editing, Funding acquisition. All authors have read the manuscript and approved its submission.

Acknowledgement

The authors thank the Guangdong Provincial Key Laboratory of Spine and Spinal Cord Reconstruction for its support and all investigators whose studies are cited in this article.

Data Availability

The uncropped immunoblot images are provided in Additional file 1. Raw qPCR Ct values and immunoblot band-intensity data are available from the corresponding author upon reasonable request.

References

1. Miyakawa H, Woo SK, Dahl SC, Handler JS, Kwon HM. Tonicity-responsive enhancer binding protein, a rel-like protein that stimulates transcription in response to hypertonicity. Proc Natl Acad Sci U S A. 1999;96:2538–42. 10.1073/pnas.96.5.2538.

2. Cheung CY, Huang TT, Chow N, Zhang S, Zhao Y, Chau MP, et al. Unconventional tonicity-regulated nuclear trafficking of NFAT5 mediated by KPNB1, XPOT and RUVBL2. J Cell Sci. 2022;135:jcs259280. 10.1242/jcs.259280.
3. Khandwala CB, Sarkar P, Schmidt HB, Ma M, Pusapati GV, Lamoliatte F, et al. Direct ionic stress sensing and mitigation by the transcription factor NFAT5. Sci Adv. 2025;11:eadu3194. 10.1126/sciadv.adu3194.
4. Ono M, Izumi Y, Maruyama K, Yasuoka Y, Hiramatsu A, Aramburu J, et al. Characterization of gene expression in the kidney of renal tubular cell-specific NFAT5 knockout mice. Am J Physiol Ren Physiol. 2024;326:F394–410. 10.1152/ajprenal.00233.2023.
5. Woo SK, Lee SD, Na KY, Park WK, Kwon HM. TonEBP/NFAT5 stimulates transcription of HSP70 in response to hypertonicity. Mol Cell Biol. 2002;22:5753–60. 10.1128/MCB.22.16.5753-5760.2002.
6. Kang K, Liao X, Li Q, Chen J, Niu Y, Zeng Y, et al. A novel tonicity-responsive microRNA miR-23a-5p modulates renal cell survival under osmotic stress through targeting heat shock protein 70 HSPA1B. Am J Physiol Cell Physiol. 2021;320:C225–39. 10.1152/ajpcell.00441.2020.
7. Jia G, Fu Y, Zhao X, Dai Q, Zheng G, Yang Y, et al. N6-methyladenosine in nuclear RNA is a major substrate of the obesity-associated FTO. Nat Chem Biol. 2011;7:885–7. 10.1038/nchembio.687.
8. Zhou J, Wan J, Gao X, Zhang X, Jaffrey SR, Qian SB. Dynamic m6A mRNA methylation directs translational control of heat shock response. Nature. 2015;526:591–4. 10.1038/nature15377.
9. Meyer KD, Patil DP, Zhou J, Zinoviev A, Skabkin MA, Elemento O, et al. 5' UTR m6A promotes cap-independent translation. Cell. 2015;163:999–1010. 10.1016/j.cell.2015.10.012.
10. Li Q, Liu J, Guo L, Zhang Y, Chen Y, Liu H, et al. Decoding the interplay between m6A modification and stress granule stability by live-cell imaging. Sci Adv. 2024;10:eadp5689. 10.1126/sciadv.adp5689.
11. Livak KJ, Schmittgen TD. Analysis of relative gene expression data using real-time quantitative PCR and the 2^(−ΔΔCT) method. Methods. 2001;25:402–8. 10.1006/meth.2001.1262.
12. Jovanovic M, Rooney MS, Mertins P, Przybylski D, Chevrier N, Satija R, et al. Dynamic profiling of the protein life cycle in response to pathogens. Science. 2015;347:1259038. 10.1126/science.1259038.
13. Li C, Liu Z, Fu C, Li H, He T, Wu G, et al. Hypoxia-induced degradation of FTO promotes apoptosis by unmasking RACK1-mediated activation of MTK1-JNK1/2 pathway. J Adv Res. 2025;77:137–53. 10.1016/j.jare.2025.01.019.
14. Cai Q, Ferraris JD, Burg MB. Greater tolerance of renal medullary cells for a slow increase in osmolality is associated with enhanced expression of HSP70 and other osmoprotective genes. Am J Physiol Ren Physiol. 2004;286:F58–67. 10.1152/ajprenal.00037.2003.
15. Mauer J, Luo X, Blanjoie A, Jiao X, Grozhik AV, Patil DP, et al. Reversible methylation of m6Am in the 5' cap controls mRNA stability. Nature. 2017;541:371–5. 10.1038/nature21022.
16. Wei J, Liu F, Lu Z, Fei Q, Ai Y, He PC, et al. Differential m6A, m6Am, and m1A Demethylation Mediated by FTO in the Cell Nucleus and Cytoplasm. Mol Cell. 2018;71:973–e9855. 10.1016/j.molcel.2018.08.011.

17. Zhang X, Wei LH, Wang Y, Xiao Y, Liu J, Zhang W, et al. Structural insights into FTO's catalytic mechanism for the demethylation of multiple RNA substrates. Proc Natl Acad Sci U S A. 2019;116:2919–24. 10.1073/pnas.1820574116.
18. Shimanski B, Marín JF, Warminski M, Eluwawalage KDA, Calzini LO, McKeon RM, et al. RNA Demethylase FTO Uses Conserved Aromatic Residues to Recognize the mRNA 5' Cap and Promote Efficient m6Am Demethylation. J Biol Chem. 2026;302:113573. 10.1016/j.jbc.2026.113573.
19. Kuschman HP, Palczewski MB, Hoffman B, Menhart M, Wang X, Glynn S, et al. Nitric oxide inhibits FTO demethylase activity to regulate N6-methyladenosine mRNA methylation. Redox Biol. 2023;67:102928. 10.1016/j.redox.2023.102928.
20. Bustin SA, Ruijter JM, van den Hoff MJB, Kubista M, Pfaffl MW, Shipley GL, et al. MIQE 2.0: Revision of the Minimum Information for Publication of Quantitative Real-Time PCR Experiments Guidelines. Clin Chem. 2025;71:634–51. 10.1093/clinchem/hvaf043.

Figures

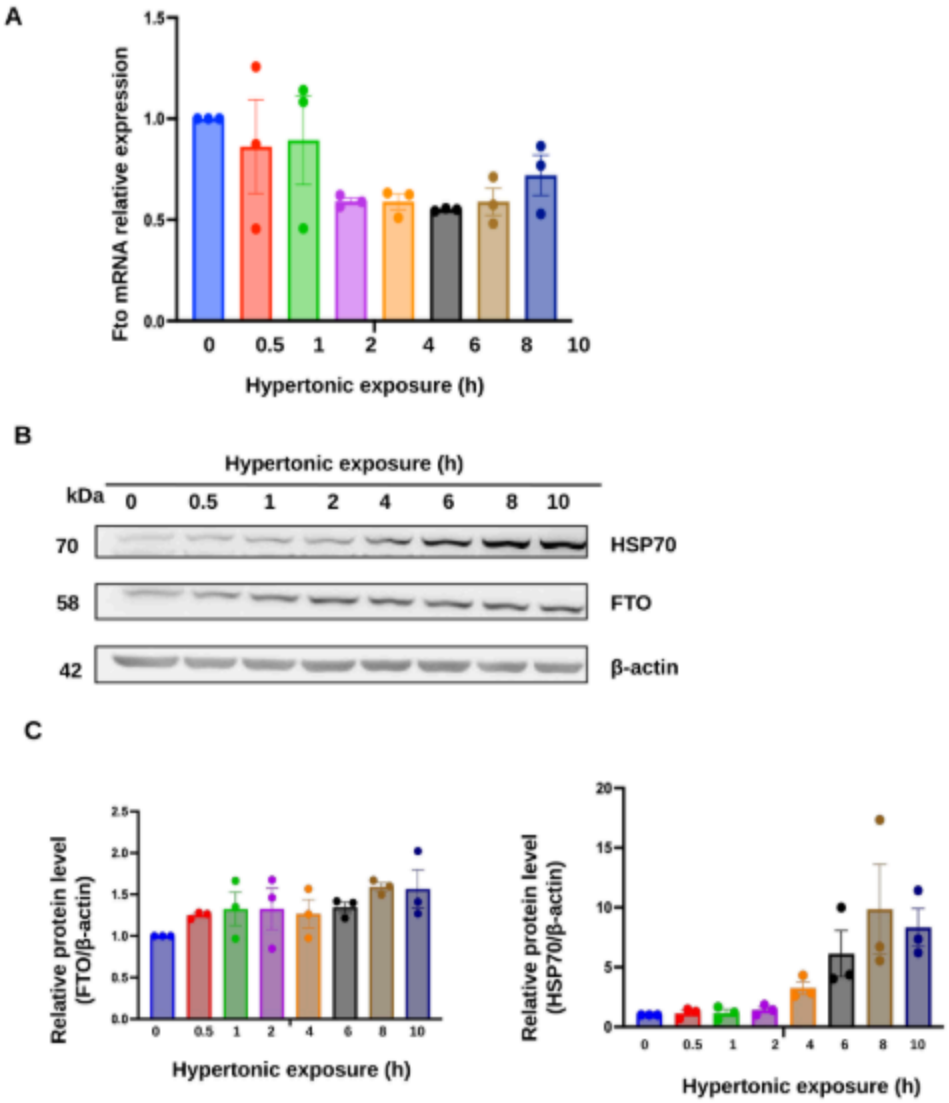

Figure 1

Temporal profiles of Fto mRNA and FTO and HSP70 proteins during hypertonic exposure. (A) Fto mRNA at 0, 0.5, 1, 2, 4, 6, 8 and 10 h, normalized to Rpl14 and calibrated to the corresponding 0 h sample. (B) Representative HSP70, FTO and β-actin immunoblots from biological replicate 1 at the same eight time points. (C) Protein quantification: FTO, left; HSP70, right. Each protein was normalized to β-actin and calibrated to its corresponding 0 h value. HSP70 time-course measurements were newly performed for this study. Each point represents one independent biological experiment; bars show mean ± SEM, n = 3. No inferential significance testing was performed. Additional file 1 provides uncropped immunoblots for all three biological replicates and identifies the exposure time for each displayed lane.

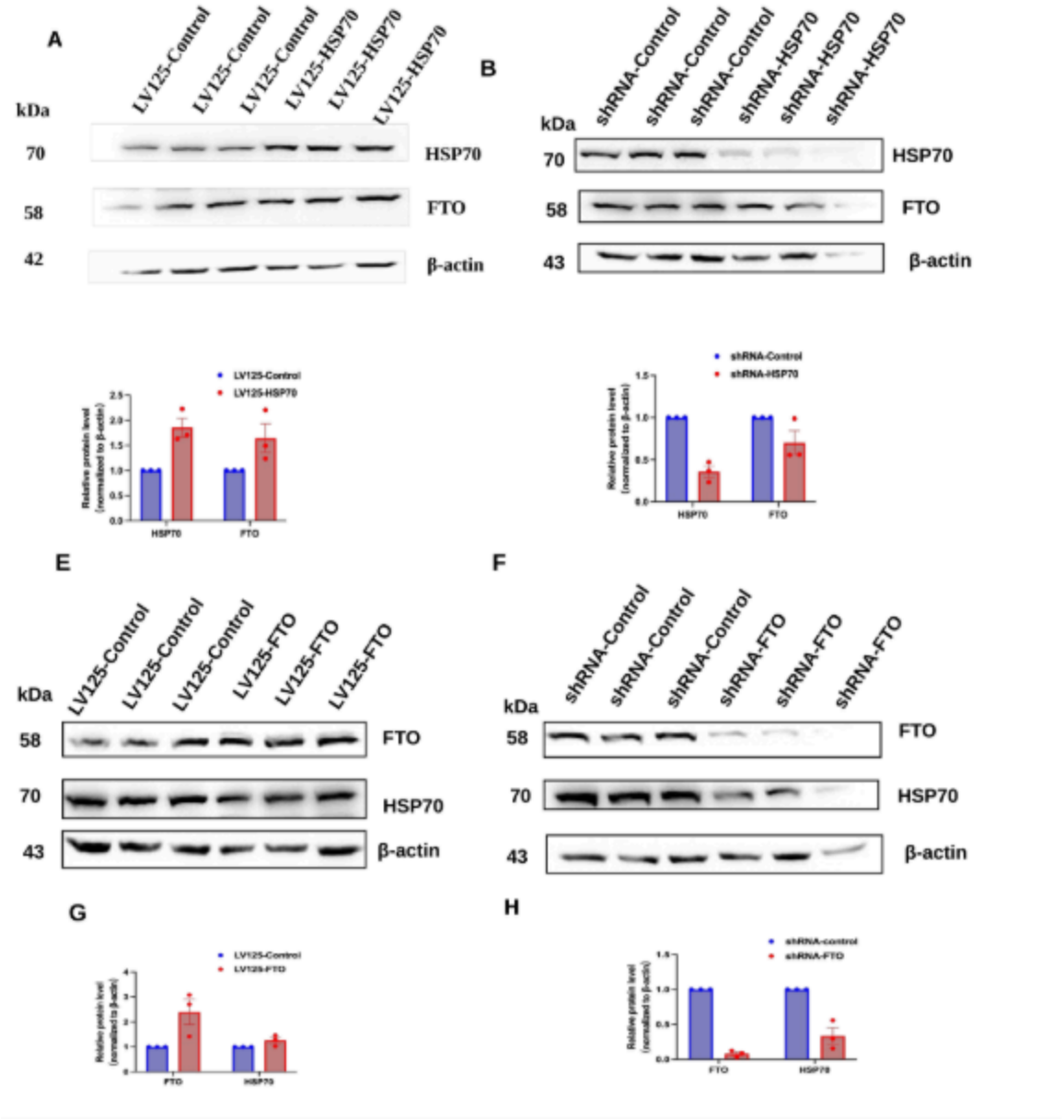

Figure 2

FTO and HSP70 protein abundance following reciprocal perturbation under isotonic conditions. In panel A, the three LV125-Control lanes precede the three LV125-HSP70 lanes. Panels A and B show immunoblots after HSP70 overexpression and knockdown, respectively, with corresponding quantification in C and D. Panels E and F show immunoblots after FTO overexpression and knockdown, respectively, with corresponding quantification in G and H. Cells were harvested 48 h after transfection under isotonic conditions. Each protein was normalized to matched β-actin and calibrated to its matched vector or shRNA control within the biological experiment. Each point represents one independent biological experiment; bars show mean ± SEM, n = 3. No inferential significance testing was performed. Additional file 1 identifies the group and biological replicate (R1–R3) for the displayed lanes.

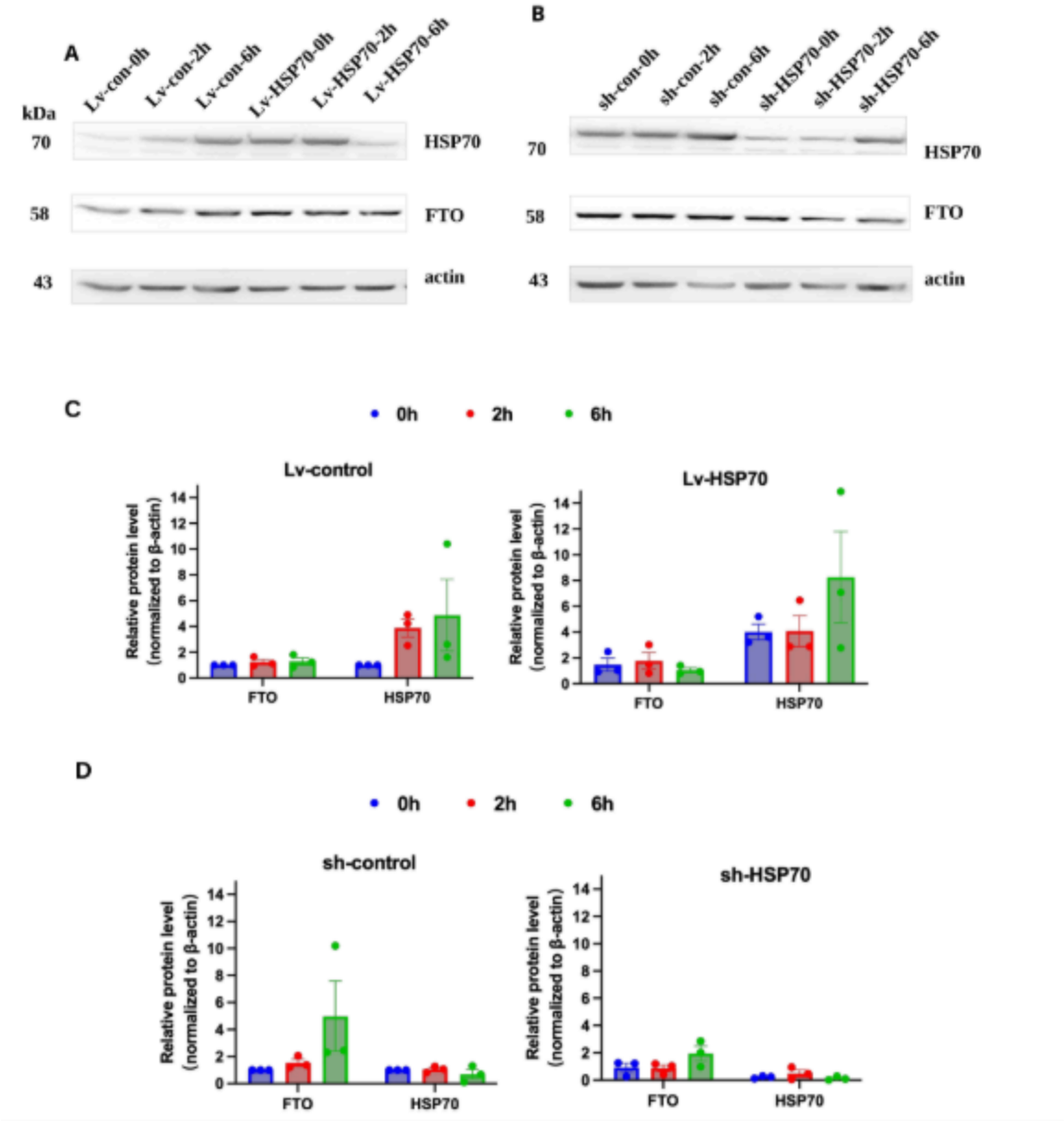

Figure 3

FTO and HSP70 protein profiles during hypertonic exposure following HSP70 perturbation. (A,B) Representative immunoblots from biological replicate 1 following HSP70 overexpression and knockdown, respectively, at 0, 2 and 6 h. (C) Overexpression-series quantification: LV-Control, left; LV-HSP70, right. (D) Knockdown-series quantification: sh-Control, left; sh-HSP70, right. Each target protein was first normalized to matched β-actin. Values for both groups in C were then divided by the LV-Control 0 h value for that protein in the corresponding experiment; values for both groups in D were divided by the corresponding sh-Control 0 h value. Intervention groups were not calibrated to their own 0 h. Thus, intervention-group baseline values need not equal 1, and relative baseline differences are retained. Each point represents one independent biological experiment; bars show mean ± SEM, n = 3. No inferential significance testing was performed. For replicates 2 and 3 in panels C and D, β-actin was measured on separate blots prepared from the same lysates and matched by sample (Additional file 1). Additional file

1 provides uncropped immunoblots for all three biological replicates and identifies the treatment group and exposure time for each displayed lane.

Supplementary Files

This is a list of supplementary files associated with this preprint. Click to download.

- Additionalfile1.pdf